

# Identification of a Novel Polyomavirus in a Pancreatic Transplant Recipient With Retinal Blindness and Vasculitic Myopathy

Nischay Mishra,<sup>1</sup> Marcus Pereira,<sup>2</sup> Roy H. Rhodes,<sup>3</sup> Ping An,<sup>4</sup> James M. Pipas,<sup>4</sup> Komal Jain,<sup>1</sup> Amit Kapoor,<sup>1</sup> Thomas Briesse,<sup>1</sup> Phyllis L. Faust,<sup>5</sup> and W. Ian Lipkin<sup>1</sup>

<sup>1</sup>Center for Infection and Immunity, and <sup>2</sup>Division of Infectious Diseases, Columbia University, New York, New York; <sup>3</sup>Pathology and Laboratory Medicine, Rutgers University, New Brunswick, New Jersey; <sup>4</sup>Department of Biological Sciences, University of Pittsburgh, Pittsburgh, Pennsylvania and <sup>5</sup>Pathology and Cell Biology, Columbia University, New York, New York

**Background.** A 33-year-old pancreatic transplant recipient developed weakness, retinal blindness, and necrotic plaques on her face, scalp, and hands.

**Methods.** A muscle biopsy was analyzed by light and electron microscopy and high-throughput nucleic acid sequencing.

**Results.** The biopsy revealed microthrombosis and viral particles in swollen endothelial cell nuclei. High-throughput sequencing of nucleic acid revealed a novel polyomavirus. In situ hybridization confirmed the presence of the polyomavirus in endothelial cells at sites of myositis and cutaneous necrosis.

**Conclusions.** New Jersey polyomavirus (NJPyV-2013) is a novel polyomavirus that may have tropism for vascular endothelial cells.

**Keywords.** virus discovery; polyomavirus; immunosuppression; transplantation; vasculitis; myositis.

## SUBJECT, MATERIALS AND METHODS

A 33-year-old woman was admitted with 3-week history of fatigue, myalgias, decreasing visual acuity, and progressive weakness. Her medical history was notable for Type 1 diabetes mellitus, peripheral neuropathy, and retinopathy leading to pancreas transplantation 11 months earlier. The transplant was complicated by cytomegalovirus viremia treated with

valganciclovir. She lived in Hoboken, New Jersey, until flood damage during Superstorm Sandy in October of 2012 forced her to evacuate through floodwaters. Her illness began 2 weeks thereafter. Her medications included prednisone 2.5 mg daily, mycophenolic acid 180 mg twice daily, and tacrolimus 6 mg twice daily. She had no history of international travel or illicit drug use, minimal exposure to domestic animals and did not recall exposure to nonhuman primates.

On admission she was afebrile, had diffuse weakness, decreased visual acuity, and a white blood cell count of 1800/mm<sup>3</sup>. Her creatine kinase was initially normal but increased, peaking at over 8000 U/L. Assays of serum by polymerase chain reaction (PCR) for human immunodeficiency virus, Epstein-Barr virus, parvovirus, and cytomegalovirus sequences, and for antibodies to influenza, adenovirus, mycoplasma, human T-lymphotropic viruses, and human herpesvirus 6 were negative. Electrophysiology revealed polyneuropathy in her lower extremities and widespread myopathy. A biceps biopsy showed vasculitis and microthrombosis in endomysial capillaries, large hyperchromatic vascular endothelial cell nuclear atypia, myonecrosis, myositis, and chronic myofiber atrophy (Figure 1A–C). Immunostaining for cytomegalovirus, herpes simplex virus, adenovirus, and BK and JC virus were negative.

A 5-day course of intravenous methylprednisolone 500 mg per day was initiated, yet weakness persisted and her vision deteriorated to detection of only bright light. Retinal mapping showed changes consistent with acute macular ischemia due to thrombosis. Anticoagulation therapy was initiated for possible antiphospholipid antibody syndrome, and she was transferred to another hospital for plasmapheresis.

On admission, she was alert, afebrile, had blanching erythema associated with necrotic plaques on her face, scalp, and hands, symmetric weakness in her extremities, decreased vibratory sensation, absent deep tendon reflexes, and could detect only bright light. Her ophthalmological exam showed bilateral optic neuropathy and retinal vascular occlusions bilaterally, in a pattern consistent with compromise of both the venous and arterial systems. A skin biopsy showed necrotizing dermatopathy (Figure 1J and 1K).

She was continued on intravenous methylprednisolone and began a 5-day course of plasmapheresis. Her muscle strength gradually increased; however, vision did not recover.

When PCR analyses of a biceps muscle biopsy for cytomegaloviruses, enteroviruses, cardioviruses, human polyomaviruses, parvovirus B19, mycoplasma, and herpesviruses failed to yield a causative agent, we pursued unbiased high-throughput

Received 8 April 2014; accepted 21 April 2014.

Correspondence: W. Ian Lipkin, MD, 722 West 168th St, 17th Fl, New York, NY 10032 (wil2001@columbia.edu).

The Journal of Infectious Diseases

© The Author 2014. Published by Oxford University Press on behalf of the Infectious Diseases Society of America. All rights reserved. For Permissions, please e-mail: journals.permissions@oup.com.

DOI: 10.1093/infdis/jiu250

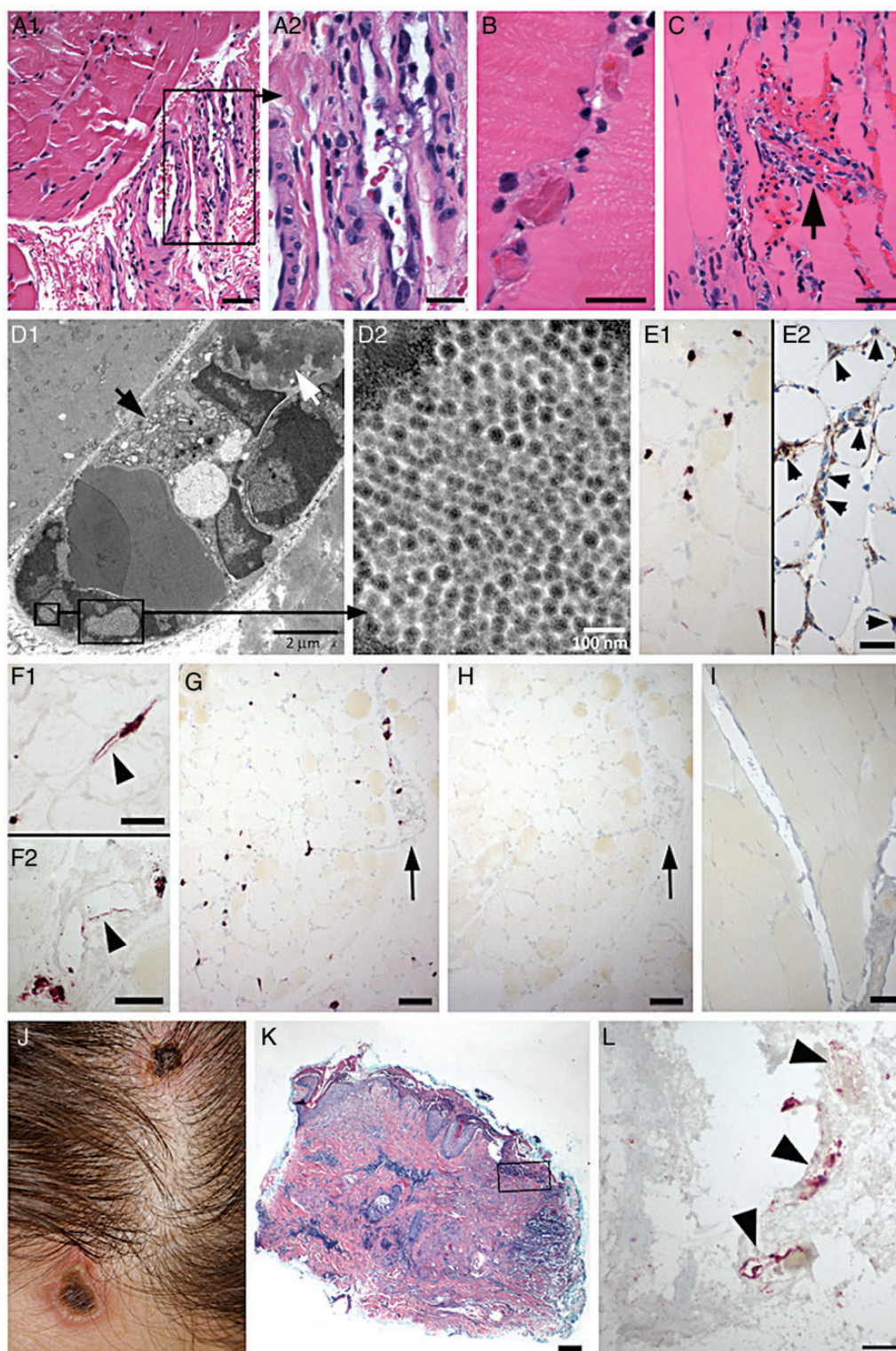


**Figure 1.** Pathologic findings in deltoid muscle and skin lesions. *A–H*, patient muscle; *I*, noninfected control muscle; *J–L*, skin lesions. *A*, Prominent endothelial cell nuclear atypia in small perimysial venules (*A1*). Boxed area in *A1* is enlarged in *A2*. There are only mild changes in the muscle in this focus, with mild fiber size variations and slightly increased cellularity in endomysium (*A1*), reflecting minimal inflammatory cell infiltration. *B*, Frequent intravascular microthrombi identified in endomysial capillaries. *C*, Endomysial capillary vascular destruction (*arrow*), with neutrophilic infiltration, nuclear fragmentation, and microhemorrhage. Marked endothelial cell atypia in adjacent capillaries and a prominent inflammatory cell infiltrate in endomysium. *D*, Electron microscopy demonstrates marked endomysial capillary damage, with atypical endothelial cell nuclei, swollen cytoplasm with numerous organelles (*D1*, black arrow), and an intravascular fibrin thrombus (*D1*, white arrow). Intranuclear viral inclusions were identified (boxed regions in *D1*), with a loose



sequencing (Ion Torrent, Life Sciences). Total nucleic acids (TNA) were extracted from sections of FFPE muscle tissue. Following DNase treatment and rRNA depletion (human Ribozero Magnetic Kit, Epicentre), approximately 450 nanograms of RNA were subjected to first and second strand complementary DNA (cDNA) synthesis. Following cDNA fragmentation and addition of barcodes and adaptors, libraries were amplified by PCR for sequencing using the Ion Personal Genome Machine (PGM) System. A total of 491 858 reads were obtained with a mean read length of 153 nucleotides (nt). Nucleotide sequence analysis (BLASTn) was uninformative; however, amino acid analysis (BLASTx) revealed 61 reads ranging from 98 to 276 base pairs (bp) with 75%–80% homology to chimpanzee polyomaviruses.

The double-stranded DNA viral genome, comprising 5108 bp, was cloned by PCR. Based on computational analyses and sequence homology with existing polyomavirus proteins, we predicted that the genome of the novel virus is capable of encoding capsid proteins VP1, 2, and 3 from the late region, as well as 3 alternative transcripts, LT, ST, and AT from the early region (Figure 2A). Phylogenetic analysis based on whole genome sequences (Figure 2B), LT and ST protein sequences (Supplementary Figure 1), as well as VP1 and VP2 protein sequences (Supplementary Figure 2) showed that NJPyV-2013 is most closely related to chimpanzee polyomavirus among all current reference polyomaviruses. Given an 80.7% overall nucleotide homology to chimpanzee polyomavirus, it meets criteria for classification as a novel polyomavirus, tentatively named New Jersey polyomavirus 2013 (NJPyV-2013, GenBank accession number KF954417).

The early pre-messenger RNA (mRNA) transcripts of polyomaviruses undergo alternative splicing to produce multiple transcripts [1, 2]. We predicted 3 T antigen transcripts based on splicing signals and protein sequence homology (Figure 2C and 2D). The structure of the predicted LT, ST, and AT transcripts are shown in Figure 2C. The potential functional domains of their corresponding proteins are illustrated in Figure 2D. To confirm the expression of the predicted transcripts at the RNA level, total RNA was isolated from the patient's muscle tissue. Primers flanking the potential splice sites were designed (Figure 2A and 2C, sequences of the primers are listed in Supplementary Table 1) and used in PCR to amplify the specific

DNA fragments corresponding to LT, ST, and AT. The sizes of the PCR products correlated with our predictions for the 3 early mRNAs (Figure 2E). The PCR products were further verified by DNA sequencing, which confirmed the specific splice junctions for LT, ST, and AT. VP1, VP2, VP3, ST antigen, and LT antigens have 78%–82% amino acid homology to the chimpanzee polyomaviruses. The AT antigen, comprising 299 amino acids, appears to be unique to NJPyV-2013.

Quantitative PCR (qPCR) of nucleic acid extracts of formalin fixed paraffin embedded (FFPE) sections indicated the presence of  $3.9 \times 10^{11}$  copies/cm<sup>3</sup> of viral DNA in muscle tissue and  $1.72 \times 10^7$  copies/cm<sup>3</sup> of viral DNA in skin lesions.

Electron microscopy of the muscle biopsy revealed intravascular fibrin thrombosis, endomysial capillary damage, and large atypical endothelial cell nuclei (Figure 1D1) that contained 36–44 nanometers structures organized in loose crystalloid arrays that were consistent in size and morphology with polyomavirus particles (Figure 1D1 and 1D2). In situ hybridization to genomic sequences comprising 517, 523, and 552 nucleotides of VP1 (2030–2546 nt), VP2 (407–929 nt), and small T antigen (4555–5107 nt), respectively, indicated the presence of virus in endothelial cells in muscle (Figure 1E1, F1, F2, 1G) and skin (Figure 1L). The identity of NJPyV-positive cells as endothelial was confirmed by CD34 immunostaining (Figure 1E2). The specificity of NJPyV-2013 in situ hybridization was confirmed by absence of signal when an enterovirus probe was used on an adjacent muscle biopsy section (Figure 1H) or the NJPyV-2013 probe was used on muscle section from a noninfected patient (Figure 1I).

Following discharge for rehabilitation the patient continued to improve in motor strength but did not recover vision. Blood collected 10 months after the onset of illness revealed  $1.6 \times 10^5$  copies/mL of viral DNA in serum. Complete genome sequencing indicated no mutations with respect to the initial NJPyV-2013 cloned from the muscle biopsy. Polyomavirus sequences were not detected in a pretransplant serum sample, in DNA from the donor pancreas or in banked sera from 35 multiple transfusion patients from the New York Blood Center, 15 rhesus macaques in a local research facility, the patient's roommate in Hoboken, her sexual partner, and other healthy controls. Her dosage of immunosuppressive medication was reduced without compromise in graft function.

*Figure 1 continued.* crystalloid arrangement (D2). Viral particles are spherical with a core of medium density, and measure 36–44 nm in diameter (D2). E–I, In-situ hybridization with New Jersey polyomavirus (NJPyV-2013) probe (E, G, I) or enterovirus probe (H). NJPyV-2013 positive nuclei in endomysium (E1) are identified as endothelial cells by immunostain with CD34 in adjacent section (E2, small arrows). Labeled nuclei are often enlarged, and endothelial cells may have cytoplasmic labeling (arrowheads, F1, endomysial capillary; F2, perimysial venule). There is widespread vascular labeling with NJPyV-2013 probe (G) in endomysium and in perimysium (arrow, G). In situ hybridization with enterovirus probe (H) shows no labeling in an adjacent section (arrow, perimysial vessel, as in G). No labeling by NJPyV-2013 virus probe in muscle biopsy from noninfected patient (I). J, Blanching erythematous necrotic plaques on scalp and forehead. K, Scalp skin biopsy demonstrates epidermal erosion, multiple foci of dermal necrosis, and marked chronic perivascular inflammatory infiltrates. L, In situ hybridization with NJPyV-2013 probe (near boxed region in panel K) labels endothelial cell profiles (arrowheads) in the superficial dermis. Panels A–C, K, Hematoxylin-eosin stain. Scale bars: A1, C, E1, E2, F1, F2, I, 50  $\mu$ m; A2, B, L, 25  $\mu$ m; G, H, 100  $\mu$ m; K, 200  $\mu$ m.

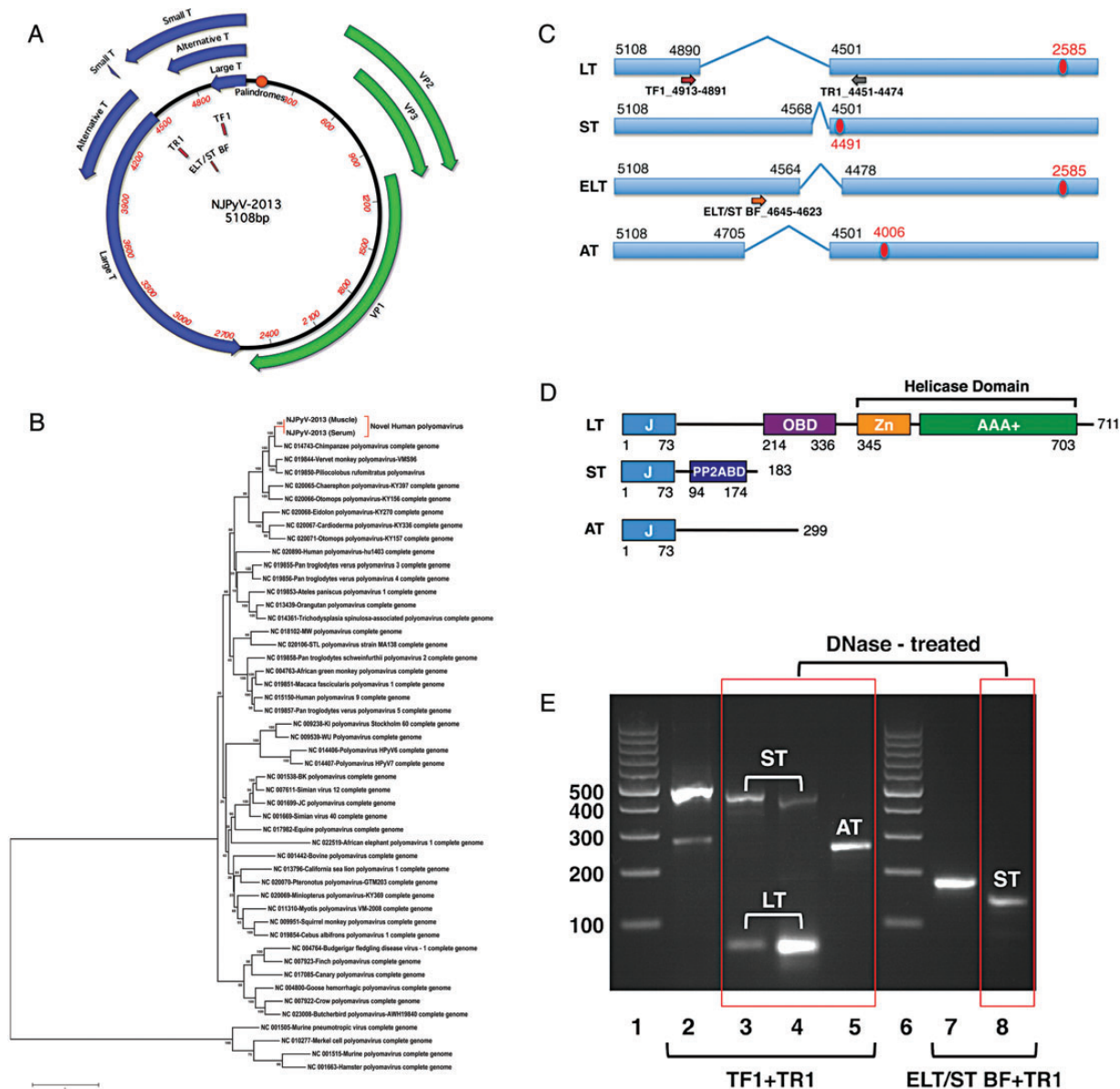


**Figure 2.** Molecular biology of New Jersey polyomavirus. **A**, Genome annotation. The double stranded DNA genome of NJPyV-2013 is 5108 base pairs in length. The coding sequences of the 3 capsid proteins VP1, VP2, and VP3 are represented by green hollow arrows. The reverse strand in the early region may have capacity for coding multiple transcripts by alternative pre-mRNA splicing. The coding sequences of several T antigens including large T (LT), small T (ST), and novel T (alternative T, AT) are indicated by blue hollow arrows. The expression of LT, ST, and AT transcripts were confirmed by PCR using RNA isolated from patient's muscle tissue. Positions of the primers TF1, TR1, and ELT/ST BF that were used for PCR detection were indicated with red bars inside the circular map. The overlapping palindrome repeats of "GAGGC" are indicated with an orange circle. **B**, Whole genome phylogenetic analysis. The phylogenetic tree was constructed using maximum likelihood method and bootstrap value 500 using the Tamura-Nei model. Results showed chimpanzee polyomavirus as the most closely related species. **C**, Early region transcription. Prediction of potential alternative transcripts of T antigens including large T (LT), small T (ST), extra-long T (ELT) and novel T (alternative T, AT). The predictions were made based on conserved splicing signals and amino acid sequences between chimpanzee polyomavirus and New Jersey polyomavirus. Red ovals indicate stop codons. **D**, Domain structure of NJPyV-2013T antigens. The potential functional domains and domain boundaries of LT, ST, and AT were predicted based on Clustal Omega alignments against the SV40 LT and ST sequences. **E**, Reverse transcription PCR amplification and DNA sequencing verification of LT, ST, and AT transcripts. Lane 1 and 6 DNA ladders. Lanes 3, 4, 5, and 8 (highlighted in red boxes) show PCR products corresponding to various T antigen transcripts. Lanes 2 and 7 are controls without DNase-treatment, which produced larger PCR products containing the unspliced intron. Abbreviations: mRNA, messenger RNA; PCR, polymerase chain reaction.

## DISCUSSION

Polyomaviruses are small nonenveloped double-stranded DNA viruses found in a wide range of mammalian and avian species. Serosurveys indicate that infection with the 2 polyomaviruses most commonly associated with human illness, BK and JC viruses, occurs in early life with an exposure prevalence over 75% in adults [3]. Human polyomavirus infection is typically asymptomatic or causes only mild respiratory disease [4]. However, BK and JC virus infection can persist throughout the life course and reactivate with immunosuppression from pregnancy, HIV/AIDS, cancer, organ transplantation, or multiple sclerosis treatment [4]. Reactivation has been implicated in renal transplant allograft failure where BK virus commonly infects renal tubular epithelium but may also replicate in endothelial cells causing vasculopathy [5]. A hemorrhagic cystitis due to BK is reported in allogeneic hematopoietic stem cell transplant recipients [6]. JC virus infection of oligodendrocytes is implicated in progressive multifocal leukoencephalopathy, a fatal demyelinating disorder. A polyomavirus has also been implicated in Merkel cell carcinoma, a rare skin cancer [7].

In the 50 years since the first human polyomavirus (JCPyV) was discovered through electron microscopy by Rhein and Chou [8], at least 11 additional human polyomaviruses have been identified [9]. NJPyV-2013, the novel polyomavirus reported here, was identified in an organ transplant recipient with systemic vasculitis, myositis, and retinal blindness. Histopathology suggests that NJPyV-2013 was tropic for endothelial cells in this individual and may have contributed to muscle and ocular damage.

We speculate that NJPyV-2013 will ultimately be known as HPyV13-NJ2013. NJPyV-2013 is most closely related to chimpanzee polyomavirus [10]. In fact, a recent serological study predicted the presence of human polyomaviruses similar to ChPyV [11]. The origin and duration of infection in this woman is unknown. She did not recall exposure to nonhuman primates. Furthermore, no NJPyV-2013 sequences were found in her pre-transplant sera, donor tissue, or in a limited PCR serosurvey of close associates, multiple transfusion patients, and nonhuman primates. It is possible that she was persistently and asymptomatically infected prior to initiation of immunosuppressive medication. Alternatively, it is possible that she acquired the virus during her evacuation through raw sewage in the aftermath of Superstorm Sandy as sequences of other polyomaviruses associated with human disease have been identified in sewage-contaminated water [12, 13]. Whether this case represents a single transmission event or the first example of human infection will only become apparent with application of diagnostic tests for NJPyV-2013.

## Supplementary Data

Supplementary materials are available at *The Journal of Infectious Diseases* online (<http://jid.oxfordjournals.org/>). Supplementary materials consist of data provided by the author that are published to benefit the reader. The posted materials are not copyedited. The contents of all supplementary data are the sole responsibility of the authors. Questions or messages regarding errors should be addressed to the author.

## Notes

**Acknowledgments.** The authors thank Vishal Kapoor, Isamara Navarette, Maria Sanchez, and Andrew Schultz for technical support and Ellie Kahn for editorial assistance.

**Financial support.** This work was supported by the National Institutes of Health [AI057158 to W. I. L. and CA170248 to J. M. P.]; USAID PREDICT and the Defense Threat Reduction Agency (DTRA).

**Potential conflicts of interest.** All authors: No potential conflicts of interest.

All authors have submitted the ICMJE Form for Disclosure of Potential Conflicts of Interest. Conflicts that the editors consider relevant to the content of the manuscript have been disclosed.

## References

1. Abend JR, Joseph AE, Das D, Campbell-Cecen DB, Imperiale MJ. A truncated T antigen expressed from an alternatively spliced BK virus early mRNA. *J Gen Virol* **2009**; 90:1238–45.
2. Trowbridge PW, Frisque RJ. Identification of three new JC virus proteins generated by alternative splicing of the early viral mRNA. *J Neurovirol* **1995**; 1:195–206.
3. Pinto M, Dobson S. BK and JC virus: a review. *J Infect* **2014**; 68 (Suppl 1): S2–8.
4. Jiang M, Abend JR, Johnson SF, Imperiale MJ. The role of polyomaviruses in human disease. *Virology* **2009**; 384:266–73.
5. Petrosiannis-Haliotis T, Sakoulas G, Kirby J, et al. BK-related polyomavirus vasculopathy in a renal-transplant recipient. *N Engl J Med* **2001**; 345:1250–5.
6. Arthur RR, Shah KV, Baust SJ, Santos GW, Saral R. Association of BK viraemia with hemorrhagic cystitis in recipients of bone marrow transplants. *N Engl J Med* **1986**; 315:230–4.
7. Feng H, Shuda M, Chang Y, Moore PS. Clonal integration of a polyomavirus in human Merkel cell carcinoma. *Science* **2008**; 319:1096–100.
8. Zurhein G, Chou SM. Particles resembling papova viruses in human cerebral demyelinating disease. *Science* **1965**; 148:1477–9.
9. Rinaldo CH, Hirsch HH. The human polyomaviruses: from orphans and mutants to patchwork family. *APMIS* **2013**; 121:681–4.
10. Deuzing I, Fagrouch Z, Groenewoud MJ, et al. Detection and characterization of two chimpanzee polyomavirus genotypes from different subspecies. *Virol J* **2010**; 7:347.
11. Scuda N, Madinda NF, Akoua-Koffi C, et al. Novel polyomaviruses of nonhuman primates: genetic and serological predictors for the existence of multiple unknown polyomaviruses within the human population. *PLoS Pathog* **2013**; 9:e1003429.
12. Fratini M, Di Bonito P, La Rosa G. Oncogenic papillomavirus and polyomavirus in water environments: is there a potential for waterborne transmission? *Food Environ Virol* **2013**. [Epub ahead of print].
13. Sidhu JP, Ahmed W, Gernjak W, et al. Sewage pollution in urban storm-water runoff as evident from the widespread presence of multiple microbial and chemical source tracking markers. *Sci Total Environ* **2013**; 463–464:488–96.